

VI The Hot ISM

We finish our discussion of the physics of the interstellar medium with a discussion of the final phase of the ISM: hot, low-density gas. This very hot plasma is often called the “X-ray corona” of the Galaxy, by analogy with the Solar corona (which is far denser), and is thought to fill the halo of our Galaxy. Its primary tracers are absorption lines seen along lines of sight towards hot stars in nearby Local Group galaxies (e.g., the LMC and SMC) or strong extragalactic UV and X-ray sources like QSOs. These lines arise primarily in the Far UV (e.g., OVI, NV, and CIV absorption) in gas with temperatures of a few 100,000K. It is also seen in diffuse soft X-ray emission in gas hotter than 10^6 K.

This gas is heated by supernova explosions and stellar wind driven bubbles (e.g., around Wolf-Rayet stars) with typical temperatures $>10^6$ K. If the gas is in rough pressure equilibrium with the surrounding phases of the ISM, the density must be very low, of order 0.01 – 0.001 cm^{-3} . The possible existence of a “Galactic Corona” was first suggested by Lyman Spitzer in 1958, in an attempt to understand how neutral HI gas clouds might survive at high Galactic latitudes. He envisioned the hot corona as a “confining medium” in rough pressure equilibrium with the cooler neutral clouds. Later work on 3-phase models of the ISM demanded a hot “third phase” that filled much of the ISM and had properties similar to Spitzer’s Galactic corona.

The hot, low-density gas is expected to be very buoyant. Estimates of the thermal scale height range as high as 5–10kpc, so the 3-phase models envision the ISM as having hot bubbles burbling up through it, churning and mixing the cooler phases, and then the bubbles cool and rain gas back down on the disk (“Galactic Fountains”). Estimates of the volume filling factor for this gas, however, have been highly controversial, ranging from 70–80% of the volume of the ISM (for the most extreme 3-phase models that have near unity porosity, see Section I-3) to as low as 20% in modern estimates. Despite this disagreement, such hot bubbles are seen throughout the ISM. Indeed, the Sun is located in an elongated **Local Bubble** roughly 100pc across that is thought to have been carved out by a past supernova. The Local Bubble has a temperature of nearly 10^6 K, but a density of only ~ 0.005 cm^{-3} .

This section of the notes will review the basic physics of the hot ISM, but our treatment will be brief as the literature is vast but largely undigested (there are no recent review articles to fall back upon, despite recent observational advances with the advent of FUSE, Chandra, and XMM). As such, we will deal primarily with Collisional Ionization Equilibrium (CIE) as an introduction to the basic physics, and end with a brief discussion of the phenomenology of Far-UV absorption lines from highly-ionized species like OVI that trace this gas.

VI-1 Collisional Ionization Equilibrium (CIE)

Very hot gas is ionized by collisions with electrons. While technically “ionized hydrogen” (H^+) the behavior of this gas is very different than what is seen in the classical HII Regions described in Chapter 3. In HII Regions, the ionization state of the plasma is tightly coupled to the radiation field and determined by the balance between photoionization of H and recombination, while the thermal state of the plasma is determined the effect of emission-line cooling by collisionally-excited metal ions closely coupled to the local thermodynamic state (density and temperature). The atomic processes of importance (recombination and line cooling following electron-ion impact excitation) are primarily concerned the electrons in the outer “valence” shells of the atoms.

Ionization in collisionally-ionized plasmas is balanced by recombination, like we saw in the case of photoionization equilibrium. However, because both collisional ionization and recombination depend on the electron density to the first power, the ionization balance in collisionally-ionized plasmas depends only on the electron temperature to a good approximation, and it is therefore tightly coupled to the local thermodynamic state of the gas. Further, as the electron temperature increases collisional processes that involve inner shell electrons become important, and we must include the effects of dielectronic recombination and autoionization when computing the excitation state.

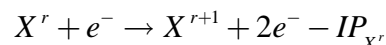
The ideal state of a hot low-density plasma is **Collisional Ionization Equilibrium** or CIE. This is often called “Coronal Equilibrium” but this is arguably less descriptive since we are rarely talking about a stellar or galactic corona per se (and the physics *are* somewhat different because of the importance of magnetic fields in classical coronae). CIE is ideal in the sense that it is rarely achieved in detail in astrophysical plasmas, for reasons we will discuss below. Despite this, it is the basic starting point of most models of hot astrophysical plasmas and it can give us useful insights into the physics of such plasmas even if CIE is not strictly achieved in detail.

There are a number of numerical codes used to predict the emergent spectrum of hot plasmas in CIE. Among the ones that you are likely to encounter in the literature or in practice are the **Raymond-Smith Code** (a small, fast code available from NASA/GSFC), **MEKAL** (Mewe-Kaastra-Liedahl) which is part of the SPEX package (formerly known as XSPEC), **APEC/APED** (Harvard HEA), and **MAPPINGS-II** (Sutherland & Dopita). Most X-ray spectral analysis packages (such as those created by the Chandra and XMM observatories) have one or other of these codes or their variants included to assist in the modeling of X-ray spectra.

It must be emphasized that CIE is not the same as LTE: in astrophysical plasmas close to CIE the level populations will be far from LTE.

Collisional Ionization

Collisional Ionization occurs when an electron collides with an ion with a relative kinetic energy greater than its ionization potential:



Collisional ionization results in a net **cooling** of the plasma because energy equal to the ionization potential is removed from the electron gas. This is the opposite of what happens in photoionization where energy absorbed from ionizing photons results in hot photoelectrons being ejected into the plasma. Also note that the inverse reaction to collisional ionization is a 3-body process, and so highly unlikely.

Collisional ionization is thus analogous to collisional excitation, and the volumetric rate of collisional excitation is expressed in terms of a collisional excitation rate, α_{coll}

$$n_e n_{X^r} \alpha_{coll}(X^r, T) = n_e n_{X^r} \int_{IP_{X^r}}^{\infty} \sigma_{coll}(E) E f(E) dE$$

Here E is the kinetic energy of the electrons, and $f(E)$ is the distribution of electron energies, usually a Maxwellian distribution if the rate of electron-electron collisions is fast enough to thermalize them (as is usually the case in astrophysical plasmas).

Collisional ionization of hydrogen and hydrogenic ions like He^+ is the only one that can be expressed analytically. For Hydrogen the rate coefficient is

$$\alpha_{coll}(H, T) = 2.5 \times 10^{-10} \left(1 + \frac{T}{78945} \right) T^{1/2} e^{-157890/T}$$

and the collisional ionization rate for hydrogenic atoms would be computed similarly. In practice, the collisional ionization cross-section is estimated empirically using multi-parameter fits to the various components of the collision cross-section, either derived from theoretical models or from actual data (e.g., collisional cross-sections measured in laboratory Tokamaks). Modeling is assisted by the fact that the cross-sections scale approximately for similar isoelectronic sequences, so once one sequence is computed, the others follow approximately if not in detail. Important cases for hot astrophysical plasmas are hydrogen-like, helium-like and lithium-like ions of various species. Details of the estimation procedures are beyond the scope of these notes, but you can find good descriptions in the classic paper by Sutherland & Dopita [1993, ApJS, 88, 253], or in Dopita & Sutherland's book *Astrophysics of the Diffuse Universe* [Chapter 5].

At very high electron energies the impacting electron can also leave the target ion in the same ionic state but very highly excited and unstable. The ion can then relax by first ejecting an electron (**autoionization**), then radiatively de-exciting into the ground level of the new ionic state. This **excitation-autoionization process** is important in heavy elements because such elements have a large number of closed inner shells and only a few electrons in the outer valance levels. Computation of the cross-sections is greatly complicated by the detailed resonance structures of such ions, which make it difficult to express the cross-sections as simple analytic approximations. Anil Pradhan's group at OSU is engaged in detailed calculation of these cross-sections if you want to see them in their full, complex glory.

Radiative and Dielectronic Recombination

Since the reverse process of collisional ionization is an unlikely 3-body process, collisional ionization will be balanced by recombination of the ion with a free electron. Since most recombinations are into excited states, there are two basic processes by which the recombined ion will relax.

The first process is **Radiative Recombination**, which we described previously in Chapter 3. A free electron recombines into an excited state and then radiatively cascades down through permitted radiative transitions into the ground state. The volumetric radiative recombination rate is:

$$n_e n_{X^{r+1}} \alpha_{RR}(X^{r+1}, T)$$

For hydrogenic atoms, the radiative recombination rate is given empirically by a formula derived by Seaton (1959, MNRAS, 119, 81):

$$\alpha_{RR}(Z, T) = 5.197 \times 10^{-14} Z \left(\frac{157890}{T/Z^2} \right)^{1/2} \left[0.4288 + 0.5 \ln \left(\frac{157890}{T/Z^2} \right) + 0.469 \left(\frac{157890}{T/Z^2} \right)^{-1/3} \right]$$

which has units of $\text{cm}^3 \text{s}^{-1}$. For non-hydrogenic atoms, various empirical approximations (usually power-law fits to available data) are used.

The second process is **Dielectronic Recombination**, which occurs when the captured electron excites an inner core electron in the target ion. The excited ion will then relax via a two-step process:

1. One of the valence electrons radiatively de-excites.
2. The ion then radiatively cascades into the ground state like in radiative recombination.

At high energies, dielectronic recombination is responsible for the emission of the **satellite lines** that are seen to accompany regular recombination lines (e.g., in the X-ray spectrum of the Solar Corona). Dielectronic recombination is important in two temperature regimes:

Low Temperature ($T \approx 1000\text{--}3000 \text{ K}$): the electron recombines into low-lying resonant states.

High Temperature ($T > 20,000 \text{ K}$): the electron recombines into a core resonant state.

At the high temperatures relevant for hot ISM phases, dielectronic recombination is the dominant process. Detailed calculations are available for only a few ions, so modelers instead exploit affinities among ions that share the same isoelectronic sequences (e.g., lithium-like ions) to make reasonable approximations when detailed calculations are not practical.

Sultana Nahar and Anil Pradhan at OSU have been computing total recombination rates *a priori* using self-consistent quantum mechanical calculations, rather than following the traditional approach of splitting total recombination into radiative and dielectronic terms computed separately using the standard empirical formulae. More advanced models are now beginning to incorporate these so-called “unified” recombination coefficients as they promise greater accuracy.

Heating and Cooling

Collisionally-ionized plasmas are heated primarily by mechanical input of energy, either from supernova blast waves or hot superwinds from massive stars (e.g., Wolf-Rayet stars), both of which can inject large amounts of energy into the ISM on relatively short timescales. While a few highly ionized species of elements can be produced by photoionization (e.g., Nv, CIV, and Si IV), the photoelectrons from these species will contribute very little to the heating. Recombination, as we saw in Chapter 3, also contributes to heating because recombination favors slower electrons, leaving the faster, hotter electrons behind in the plasma. In practice, recombination is often included in thermal balance calculations as a negative cooling term rather than in the heating side of the equation. Finally, at very high temperatures ($T > 10^8 \text{ K}$), non-relativistic Compton heating can begin to become important. Globally, heating is dominated by supernovae.

Cooling in a hot, collisionally-ionized plasma arises from the ionization process itself and from a variety of line and continuum processes:

Hydrogen & Helium Collisional Excitation

At temperatures between about 20,000 and 40,000K, collisional excitation of H^0 and He^0 followed by line emission dominates cooling in hot plasmas, with collisional excitation of He^+ becoming important above $\sim 400,000 \text{ K}$. The effectiveness of collisionally-excited H and He emission-line cooling diminishes at higher temperatures as heating from collisional ionization becomes more important.

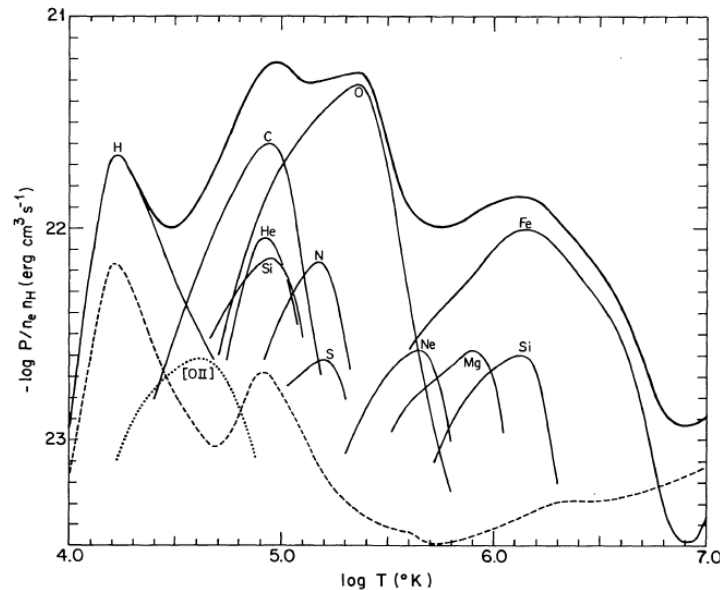
Collisional Line Cooling from Metal Ions

At low temperatures ($T < 15,000\text{K}$), as we saw in classical HII regions, forbidden lines from collisionally-excited metal ions were the most important emission-line coolants. At higher temperatures ($T > 60,000\text{K}$) contributions from collisionally-excited resonant permitted lines quickly becomes dominant, reaching a maximum cooling efficiency at temperatures around $250,000\text{K}$ depending on the metallicity of the gas. Near $100,000\text{K}$, collisional excitation of so-called “inter-system” and fine structure lines becomes important as well. Important low-density cooling species at temperatures above $100,000\text{K}$ include OVI, Si IV, CIV, SVI and NV, all of which produce strong emission lines in the Far Ultraviolet. At higher densities, visible-wavelength lines of FeX and FeXIV are observed (e.g., in the Solar Corona). All of the low-density cooling species have been seen in absorption in the hot ISM – the densities are so low that emission lines have very small emission measures are thus have such surface brightnesses they have not yet been observed directly. Searches for the highly-ionized “coronal” states of Fe, however, have only been marginally successful. In general, metal-line cooling dominates between about $40,000$ and 10^{6-7} K, depending on the metallicity of the gas.

Free-Free Continuum Cooling

At temperatures above 10^{6-7} K, free-free cooling becomes the dominant cooling mechanism and remains dominant to higher temperatures. The free-free cooling rate scales like $T^{1/2}$ and includes contributions from H, He, and metals (the latter of which have contributions scaling like the product of their relative abundances and Z^2). This cooling is manifest in the emergent spectrum as a **Thermal Bremsstrahlung Continuum** that appears at extreme-UV (EUV) and soft X-ray energies, and dominates the overall shape of the emergent spectrum of hot ionized plasmas.

The figure below shows the cooling function for lines (solid) and continuum (dashed) for a high-temperature plasma (from Gaetz & Salpeter, 1983, ApJS, 52, 155). Beyond 10^7 K, thermal continuum emission dominates the cooling, showing a $T^{1/2}$ spectrum.



Line (solid) and continuum (dashed) cooling at high T (from Gaetz & Salpeter 1983)

CIE and Astrophysical Plasmas

While collisional ionization equilibrium is an important and calculable condition, it is rarely achieved in real astrophysical plasmas. Consider the stability of hot plasmas. As we saw in our discussion of the multiphase ISM in Chapter 1, the Field Criterion for a gas to be unstable against isobaric

perturbations is $(d \ln \Lambda / d \ln T)_p < 1$. The thermal bremsstrahlung continuum cooling rate is proportional to $T^{1/2}$ and so this derivative is 0.5, meaning that the gas is formally unstable against isobaric perturbations. Such a gas should not exist in stable pressure equilibrium with other thermal phases.

That it persists at all is because the cooling times are very long at high temperatures. When the cooling is dominated by thermal bremsstrahlung, the volumetric cooling rate is

$$\Lambda \approx 3 \times 10^{-27} T_e^{1/2} \text{ erg cm}^3 \text{ s}^{-1}$$

This corresponds to a free-free cooling time of

$$\tau_{ff} \approx 5 \times 10^7 n^{-1} T_8^{1/2} \text{ years}$$

(where T_8 is the temperature in units of 10^8 K). For low-density hot ionized gas with a density of $n \approx 10^{-3} \text{ cm}^{-3}$ and $T = 10^8$ K, the cooling time is ~ 50 Gyr, longer than the Hubble Time. Further, even at lower temperatures and higher densities where the cooling time is shorter, the cooling time is still long compared to the mean time between supernovae at a given location in the Galaxy (estimated at about once every 10^{6-7} years), so the gas always stays hot and churned up by supernovae even though it is formally unstable according to the Field Criterion.

While this only establishes that the hot plasma can persist, the more pertinent question is whether it can achieve CIE. The timescale to establish collisional ionization equilibrium is

$$\tau_{CIE} = \frac{1}{n_e (\alpha_{coll} + \alpha_{rec})}$$

The denominator includes both the collisional ionization and recombination rates (the latter of which includes both radiative and dielectronic recombination). This looks very similar to the recombination time we computed for HII regions in Chapter 3. The CIE timescale must be evaluated for all relevant ions and ionization states in the gas. CIE will hold when the CIE timescale is much less than the cooling time:

$$\tau_{CIE} \ll \tau_{cool}$$

From arguments given above for high temperatures where free-free cooling dominates, we expect that this condition should hold only at very high temperatures. Detailed calculations (e.g., by Sutherland & Dopita 1993) show that CIE holds for some ions but not others given the relative contributions of those elements to emission-line cooling on the one hand, and their relevant CIE timescales on the other. For example, if only considering Iron emission-line cooling, CIE should be an excellent approximation for temperatures above 300,000K, but for Carbon emission-line cooling CIE will not occur until temperatures are well above 10^6 K, and even then it does not work so well if Carbon is mostly helium- or hydrogen-like because such states have very long recombination times, greatly increasing the CIE timescale relative to the cooling time.

In general, the assumption of CIE in the ISM will only be valid at very high temperatures of $T > 10^7$ K or so. At low temperatures, typical astrophysical plasmas significantly depart from CIE, but where the exact breakdown in CIE occurs depends on the details of the line cooling function. Detailed numerical models (e.g., by Mappings-II or SPEX) can attempt to model non-equilibrium plasmas in various ways. Such “Non-Equilibrium Ionization” or NEI models include ionizing plasmas, recombining plasmas, “thermal plus high-energy electron tail” plasmas and others. A good illustration is the set of “NEQ” models presented by Sutherland & Dopita (1993).

VI-2 The Spectrum of the Hot ISM

The emergent spectrum of the hot low-density ISM consists of the following components:

1. A thermal free-free (bremsstrahlung) continuum with significant contributions from metal ions (the amount of thermal free-free continuum scales like Z^2).
2. Bound-free continuum characterized by a large number of absorption edges from metal-ion species.
3. 2-photon continuum from de-excitation of metastable states in ions.
4. Permitted recombination lines arising from post-recombination de-excitation cascades.
5. Collisionally-excited forbidden and permitted resonance lines of metal ions.

Calculations of the emergent spectrum, either from CIE models (e.g., Raymond-Smith or MEKAL) or various kinds of non-equilibrium models (e.g., photoionized or recombined plasmas) are now done as a matter of course for modeling observations acquired with Extreme-UV or X-ray satellites. The model calculations are complicated by the necessity of including many metal ion states, many of which have only poorly determined atomic data, and by the need to include atomic processes that have strong resonant structures like autoionization resonances. Since many effects due to metal ions scale like Z^2 , rare elements can often contribute far out of proportion to their low abundances, quite unlike what we saw in HII regions. Simple H-only or H/He-only approximations like we used when examining the properties of classical photoionized HII regions are folly in the hot collisionally-ionized phases of the ISM.

Observations of the hot phases of ISM are also complicated. Most of the emission is at EUV and X-ray wavelengths and requires space-borne observatories. Recent missions like EUVE, ROSAT, ASCA, Chandra and XMM are providing us with new and important data on the hot ISM that we'll briefly review below.

ISM Opacity and the Observed Spectrum

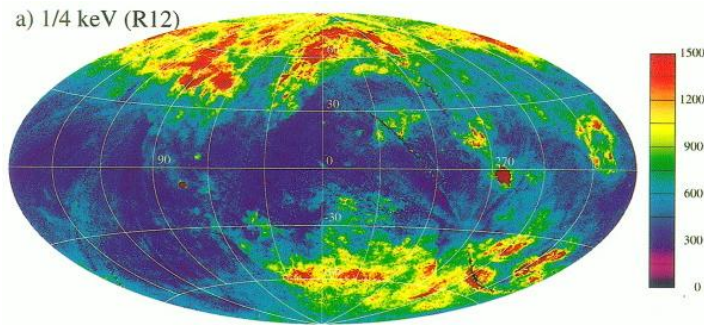
The principal complication in observing the hot ISM is that most of the radiation occurs in a part of the spectrum with significant opacity from the cool and “warm” (e.g., 10^4K) phases. In particular, photoelectric absorption by neutral hydrogen at energies above the 13.6 eV H^0 ionization threshold has a large optical depth (column-density times cross-section), as does He^0 absorption above the 24.6eV ionization edge and He^+ absorption above the 54.4eV ionization edge. The mean free path for a 13.6 eV photon in neutral H for typical ISM densities ($\sim 0.3\text{ cm}^{-3}$) is measured in parsecs. At soft X-rays energies ($\sim 0.2\text{--}1\text{ keV}$), a relatively modest H^0 column density of 10^{21} cm^{-2} , corresponding to ~ 0.5 mag of visual extinction, can effectively attenuate all soft-X-ray emission below 0.2-0.3 keV, which represents the approximate low-energy limits of the ROSAT, Chandra, and XMM X-ray telescopes.

Much of our knowledge of the local Hot ISM at EUV wavelengths not surprisingly comes from within 100pc from the Sun, an elongated region of very low density ($n_{\text{H}}\approx 0.005\text{ cm}^{-3}$) hot ($T\approx 10^6\text{ K}$) gas known as the **Local Bubble**. Because of its relatively low density, and corresponding low emission measure, most of our data comes from absorption line studies of very hot stars, primarily a handful of nearby hot white dwarf stars and B supergiant stars.

Diffuse Soft X-ray Continuum Emission

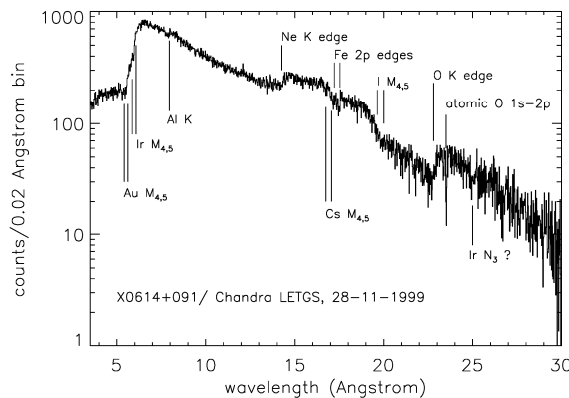
At soft X-ray energies, all-sky mapping missions, beginning with short-duration sounding rocket flights (e.g., the “Wisconsin Survey” of McCammon et al. 1983, ApJ, 269, 107), and the long-duration SAS-3 mission (Marshall & Clark 1984, ApJ, 287, 633) observed diffuse emission from the hot “coronal” phases of the ISM. The emission in the softest bands (the 130-190 eV “B” band and 160-280 eV “C” band – named for the use of Boron and Carbon detector windows, respectively) is strongly anti-correlated with the HI column density, as expected for photoelectric absorption by metals associated with the HI gas. Nonetheless, when corrected for the estimated absorption, there is a significant diffuse foreground component seen along many lines of sight consistent emission from the low-density, 10^6 K gas in the Local Bubble.

ROSAT had greater soft X-ray sensitivity and angular resolution than SAS-3, permitting the removal of most of the point sources to reveal the soft diffuse component of the Galactic ISM in greater detail (Snowden et al. 1997, ApJ, 485, 125). Using data from the softest ROSAT Bands (R1: 110-284 eV and R2: 140-284 eV), they subtracted the background sources and corrected the data for photoelectric absorption. The results (below) show a considerable local component of hot gas, with a distinct plane/halo symmetry (shown below in an Aitoff projection into Galactic Coordinates):



ROSAT 0.25keV Map of the Milky Way [from Snowden et al. 1997]

Chandra and XMM also have the ability to observe the hot phases of the ISM with significant spectral resolution. Observations towards bright X-ray continuum sources (e.g., X-ray binaries) along lines of sight through the Galactic plane show strong absorption components. For example, Chandra observations by Paerels et al. (2001, ApJ, 546, 338) show O, Ne, and Fe K- and L-shell absorption edges in the spectrum of the low-mass X-ray binary X0614+091 (the edges labeled Au, Ir, Al, Cs, and I are instrumental artifacts not interstellar features). These data are taken along a relatively low-density sight line through the Galaxy.



Diffuse Soft-X-ray absorption towards X0614+091 from Paerels et al. 2001.

Absorption Lines

Because of their low emission measure, direct detection of emission lines from the hot ISM is extremely difficult, but these species are readily visible as absorption lines towards bright UV continuum sources (usually hot stars or AGN if looking out of the plane of the Galaxy). Most of these lines are in the Far-UV region of the spectrum ($\lambda < 1100 \text{ \AA}$). This puts these lines in the regime accessible to the FUSE spacecraft, with other lines are in the Near-UV spectrum accessible by IUE and HST.

Because the lines are from collisionally ionized species, the maximum abundance of a particular ionic species occurs at a particular temperature. To a first approximation, different lines trace different temperatures. While soft X-rays trace hot gas at temperatures of $\sim 10^6$ K, the important UV absorption lines trace slightly cooler gas at temperatures of a few 100,000 K.

Important UV lines are listed below:

Species	Lines (\AA)	IP (eV)	T_{max} (K)
Si IV	1402.7, 1393.8	33.5/45.1	60,000 K
C IV	1550.8, 1548.2	47.9/64.5	100,000 K
S VI	944.5, 933.4	72.5/88.0	200,000 K
N V	1242.8, 1238.8	77.5/97.9	180,000 K
O VI	1037.6, 1031.95	113.9/138.1	300,000 K

The ionization potentials (IP) listed are those required to create/destroy this ionic state.

Of these lines, Si IV, CIV, SVI, and NV all have relatively low ionization potentials and are plausibly produced by photoionization. While in general they are tracers of gas at their respective ranges of temperatures, they are not definitive tracers of *collisionally* ionized gas. However, Si IV, CIV, and NV are all easily observed with HST (and earlier with IUE), and so are convenient lines, if ambiguous.

OVI is by far the best indicator of collisionally ionized gas at temperatures of a few 100,000 K. It is a very strong doublet resonance line, so even if it is a relatively “fragile” lithium-like ion, its large oscillator strength makes it relatively easy to observe even if the ionic abundance is small. OVI absorption in the Galactic disk shows multiple components, like seen in lower-ionization near-UV and visible-wavelength lines, showing an internal velocity dispersion of $\sim 10\text{--}15 \text{ km s}^{-1}$, consistent with thermal Doppler widths for temperatures of $\sim 300,000\text{--}400,000$ K.

The strength of OVI absorption also makes it observable outside of the Galactic disk, and provides us with our only good probe of very low-density Galactic halo “coronal” gas and hot gas associated with “high-velocity clouds” in the intergalactic regions of the Local Group (see, for example, the May 2003 ApJ Letters special issue on the FUSE survey of halo and high-velocity clouds for a detailed recent overview of the subject). With the loss of the FUSE spacecraft at the end of its rather extended life, observations of OVI are now restricted to absorption-line systems with redshifts $z > 0.068$ where they begin to enter the Far-UV window of HST at $\sim 1100 \text{ \AA}$, or from very high-redshift absorbers ($z > 2.4$) where the lines begin to enter the near-UV window ($\lambda > 3500 \text{ \AA}$) accessible from the ground (e.g., with UVES on the VLT).